Thin Solid Films 529 (2013) 222–225

Contents lists available at SciVerse ScienceDirect

Thin Solid Films

journal homepage: www.elsevier.com/locate/tsf

Effect of wavelength on the laser patterning of a cholesteric liquid crystal display electrode

C.H. Li [a,*], H.K. Lin [a,b]

[a] Laser Application Technology Center / Industrial Technology Research Institute South (ITRI South),8 Gongyan Rd., Liujia Dist., Tainan City 734, Taiwan, R.O.C.
[b] Graduate Institute of Materials Engineering, National Pingtung University of Science and Technology, 1, Shuefu Road, Neipu, Pingtung 912, Taiwan, R.O.C.

ARTICLE INFO

Available online 26 March 2012

Keywords:
Laser
Cholesteric liquid crystal
Silver electrode
Flexible display

ABSTRACT

A 1064 nm fiber laser and a 355 nm ultraviolet solid-state laser with galvanometer scanners and F-theta lenses are used to rapidly etch the silver electrode pattern of a cholesteric liquid crystal display. These results of the two laser processes are that the 1064 nm laser effectively reduces the damage to the liquid crystal layer and underlying indium tin oxide layer, and reduces the heat-affected zone of the ablated silver electrode.

1. Introduction

Flexible displays are suitable for e-books, electronic tags, electronic billboards, and other flexible electronic products. For portable applications, displays must be inexpensive, light-weight, low-power, rugged, flexible, and easy to carry [1]. Reflective cholesteric liquid crystal displays (Ch-LCDs) have low power consumption, memory, wide range, and are legible in sunlight, so it have been developed recently [2]. Ch-LCDs have bistable states, so they consume electricity only when changing the screen content [3]. Ch-LCDs can be switched between bend and splay deformation in a three-electrode configuration and have an infinite bistable lifetime [4].

Ch-LCDs have a stacked structure [5]. The substrate is a flexible transparent material. Driving electrodes are a silver electrode and an indium tin oxide (ITO) electrode. The intermediate layer is the liquid crystal layer. A driving voltage applied to the electrodes makes the liquid crystal layer switch to the different situations [6]. ITO is etched by a wet etching process, which requires many steps, including the production of a mask, photoresist, exposure, development, etching, and resist removal [7]. Furthermore, Ch-LCDs can not be exposed to organic solvents, so the traditional wet etching process is not used for electrode patterning. Most silver electrodes are patterned using screen printing technology [8]. When a Ch-LCD silver electrode layer needs to produce different graphics of product design, the electrode patterns require a re-designed stencil, which increases the process time and stencil production costs. Etching silver electrodes using laser technology is thus desirable.

Laser patterning technology requires neither a mask nor a stencil. It can effectively shorten the production process. The processing electrode resolution depends on the size of the laser spot. The resolution can reduce the spot by adjusting the optical lens, so processing width can achieve high resolution requirements [9,10]. If the laser uses direct-write techniques, the processing of complex patterns will be time-consuming. To achieve rapid processing of complex patterns, laser with a scanner can be integrated into the patterning process. With the development of laser micro-processing technology, many studies have shown that laser processing an ITO electrode can effectively etch the required electrode pattern [11–13].

A high-resolution laser can etch the silver electrode layer without damaging the ITO electrode layer [14]. However, using a 355 nm ultraviolet laser processing will lead to poor processing quality and a low processing speed. Therefore, this study compares a 1064 nm fiber laser with 355 nm solid-state laser for etching ITO electrode and silver electrode layers.

2. Experimental method

The flexible Ch-LCD is composed of a polymer dispersed cholesteric layer (BL118, Merck) and a dark layer (R-122, BASF) sandwiched between the top and bottom electrodes on a polyethylene terephthalate (PET) substrate. A 1064 nm fiber laser (SP-20P, SPI) and a 355 nm solid-state laser (AVIA355-7000, Coherent) equipped with a scanner (Scanlab) were used to pattern the silver electrode.

* Corresponding author. Tel.: +886 6 6939166; fax: +886 6 6939056.
E-mail address: chunhanli@itri.org.tw (C.H. Li).

0040-6090/$ – see front matter
doi:10.1016/j.tsf.2012.03.063

The diameter of a laser spot is related to the resolution of pattern. The diameter of the laser spot, D_0, can be calculated as:

$$D_0 = 1.22 \times \left(\frac{\lambda \times F}{n \times W_d}\right) \times M^2 \quad (1)$$

Where λ is the laser wavelength, F is the focal length, n is the refractive index, W_d is the diameter of the incident laser, and M^2 is the laser-quality factor. For the 1064 nm fiber laser, M^2 is 1.8, F is 250 mm, and W_d is 14.5 mm. For the 355 nm solid-state laser, M^2 is 1.3, F is 250 mm, and W_d is 3.5 mm. The spot diameters for the two laser systems are both 40 μm.

The change of laser processing speed is related to the overlap. With laser spot diameter D and gap distance S (processing speed / laser frequency), the overlap is calculated as:

$$Overlapping = \frac{D-S}{D} \times 100\% \quad (2)$$

Both the 1064 nm fiber laser and the 355 nm solid-state laser can effectively ablate the silver electrode of the Ch-LCD. A 40 μm spot diameter and a 40 kHz laser frequency were used for the patterning of the silver electrode. When the silver electrode was etched completely, the resistance is greater than 20 MΩ. To determine whether the underlying ITO electrode was etched, a voltage was applied. If the state of the liquid crystal can be changed and display the pattern. It means that the ITO electrode layer was not etched.

3. Results and discussion

A schematic diagram of an ablated silver electrode of a Ch-LCD is showed in Fig. 1. The thickness of the Ch-LCD structure includes ~130 μm PET flexible substrate, ~60 nm of ITO electrode layer, ~7 μm liquid crystal layer (LC) with the absorption layer (NP), and the ~16 μm silver electrode. The ablated electrode can be divided into the under-etching area (I), the etching area (II), and the over-etching area (III). In area I, the measured resistance is below 20 MΩ and the silver electrode is not etched completely. The resistance in area II, where the electrode is fully ablated, is above 20 MΩ. The state of liquid crystal changed when a voltage was applied to this area, indicating that the underlying ITO electrode was not ablated.

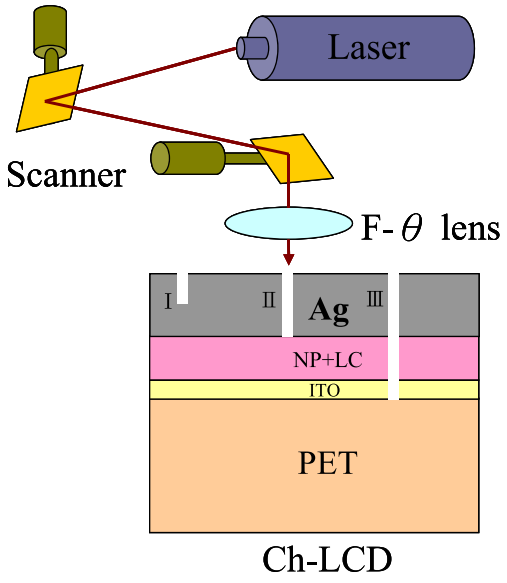

Fig. 1. Schematic diagram of laser ablation of a Ch-LCD with silver electrode.

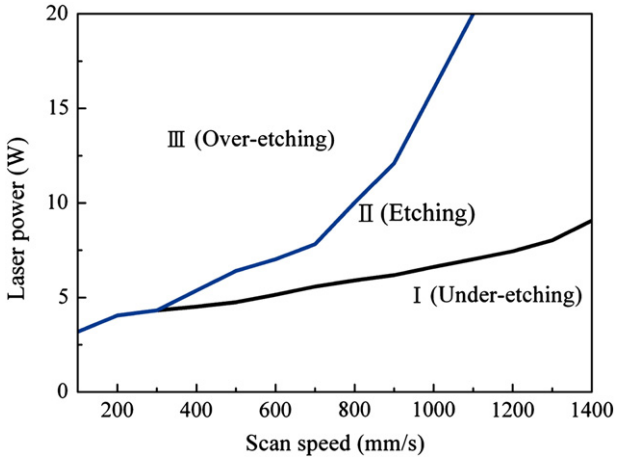

Fig. 2. Relationship between scan speed and laser power for 1064 nm fiber laser. (I under-etching area, II etching area, III over-etching area).

In area III, both the silver layer and the underlying ITO films were ablated.

The silver electrode of a Ch-LCD was ablated using the 1064 nm fiber laser with scan speeds of 100 to 1400 mm/s. Fig. 2 shows the relationship between scan speed and laser power to ablate the silver electrode. The results show that laser processing with a galvanometer can ablate the silver electrode layer without damaging the ITO electrode layer for scan speeds above 300 mm/s. When the processing speed is increased, the laser power increases, and the interval of area IIincreases. If the laser power is excessive, it will appear in area III. With excessive laser power, the underlying ITO electrode layer was also ablated, so the liquid crystal layer cannot be driven by the electric voltage (open-circuit). With an overlap of 75% and a laser power of 4.5 W, the silver electrode can be ablated. The electrode can be ablated at 1400 mm/s, but the laser power increases to 9.1 W.

The silver electrode was ablated using the 355 nm solid-state laser with scan speeds of 100 to 600 mm/s. Fig. 3 shows the relationship between scan speed and laser power. In order to avoid damaging the underlying ITO electrode layer, the scan speed must be over 100 mm/s. With a scan speed of 200 mm/s, the silver electrode was ablated at the lowest power (1.5 W). For scan speeds above 600 mm/s, the laser power increases to up to 7 W. It is apparent that to increase the scan speed, it is necessary to increase more laser power to ablate the silver electrode.

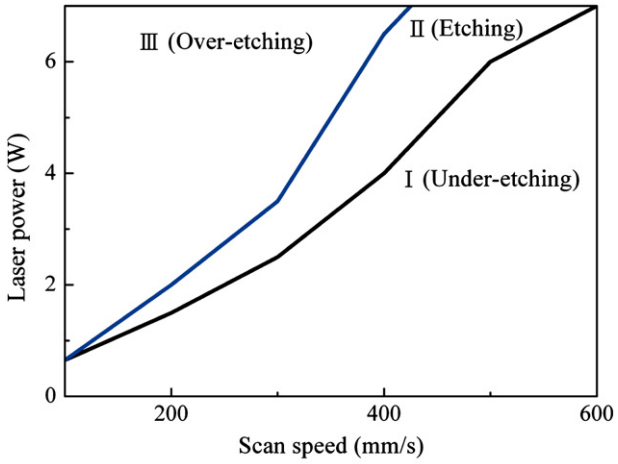

Fig. 3. Relationship between scan speed and laser power for 355 nm solid-state laser. (I under-etching area, II etching area, III over-etching area).

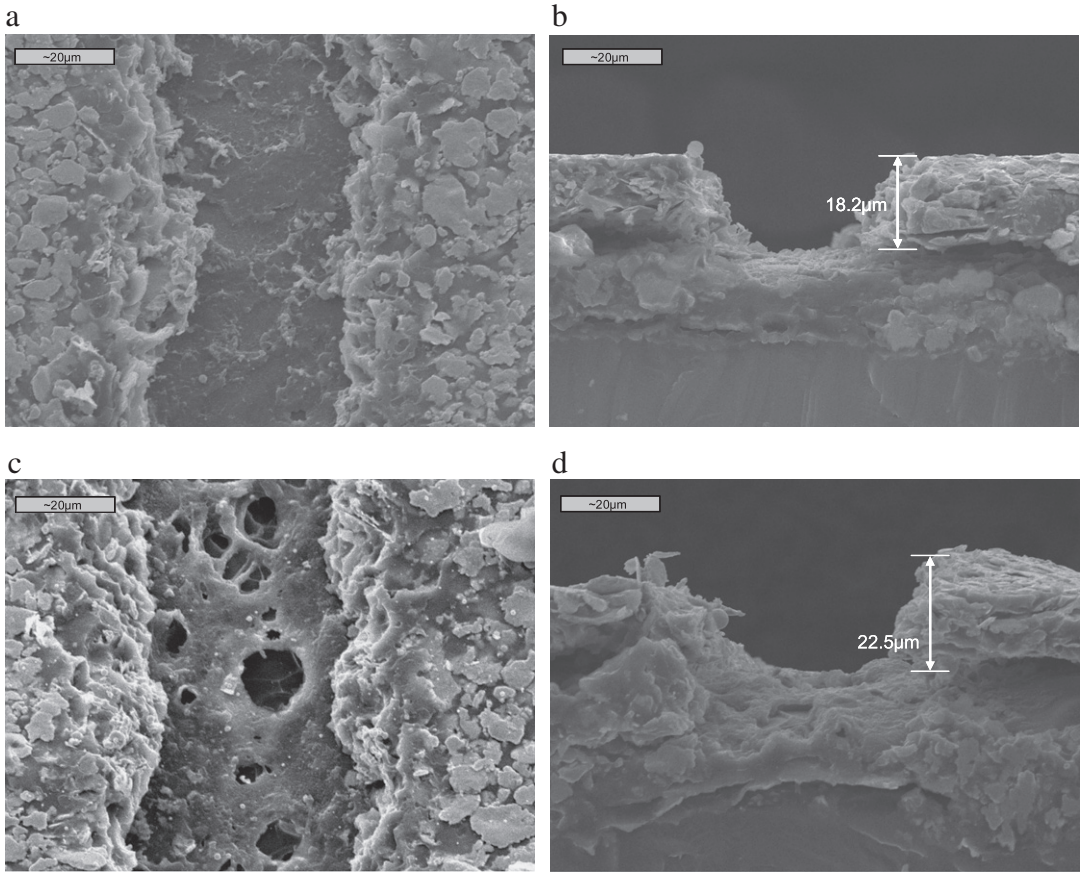

Fig. 4. SEM micrographs: (a) result of electrodes etched by 1064 nm fiber laser and (b) etching depth of 1064 nm fiber laser (cross section view) (c) result of electrodes etched by 335 nm UV laser (d) etching depth of 355 nm UV laser (cross section view).

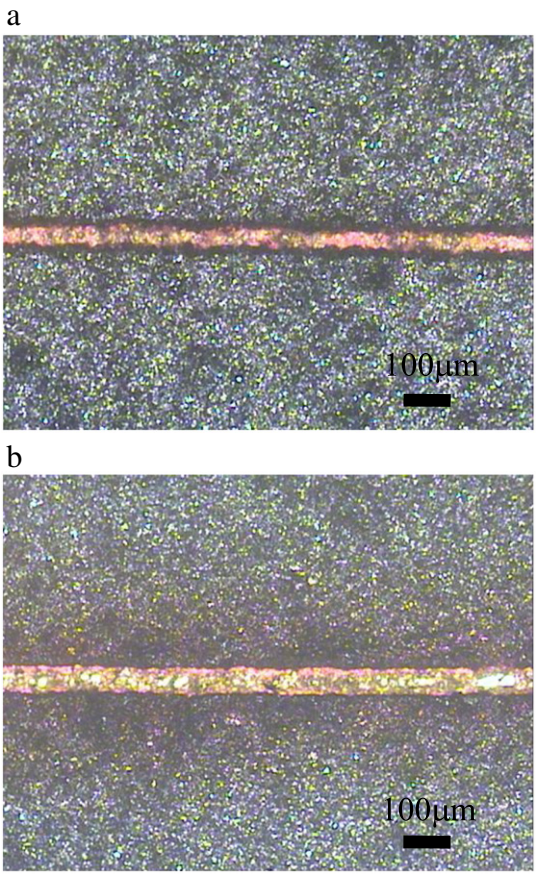

Fig. 4(a) shows that the ablated line width is about 44 μm for the 1064 nm laser with a scan speed of 500 mm/s and a laser power of 6 W. Fig. 4(b) shows that the etching depth is 18.2 μm by cross section SEM image. This experiment result is in area II. The laser only ablated the silver electrode, but it doesn't injure the underlying ITO electrode layer. Fig. 4(c) shows the experiment results in area II when the silver electrode ablated with the 355 nm laser with a scan speed of 500 mm/s and a laser power of 6 W. The ablated line width is about 42 μm. The scanning electron microscopy images show that the 355 nm solid-state laser slightly damages the ITO electrode layer. Fig. 4(d) shows that the etching depth is 22.5 μm by cross section SEM image. The 1064 nm laser reduces the damage to the ITO layer at the same condition. Fig. 5 shows the heat-affected zone around the ablated silver electrode after the laser etching process. The heat-affected zones for the 1064 nm and 355 nm lasers were 13 μm (Fig. 5(a)) and 115 μm (Fig. 5(b)), respectively. It is obvious that 1064 nm fiber laser processing silver electrode layer can effectively reduce heat-affected effect zone of the ablated silver electrode and reduce the damage to the underlying ITO layer.

Fig. 6(a) shows the silver electrode etched using the 1064 nm fiber laser with a power of 7 W and a scan speed of 1000 mm/s. 80 V was applied to the Ch-LCD. Fig. 6(b) shows the driving voltage results for a Ch-LCD with a silver electrode patterned using the 355 nm solid-state laser with a power of 5 W and a scan speed of 400 mm/s. Both lasers can ablate the silver electrode layer and reduce the damage to the ITO layer. For the different wavelength laser systems, it is obvious that the heat-affected zone using 1064 nm fiber laser is smaller than using 355 nm.

Fig. 5. OM images of electrode etched (a) with 1064 nm laser at 1000 mm/s and a power of 7 W and (b) with 355 nm laser at 400 mm/s and a power of 5 W.

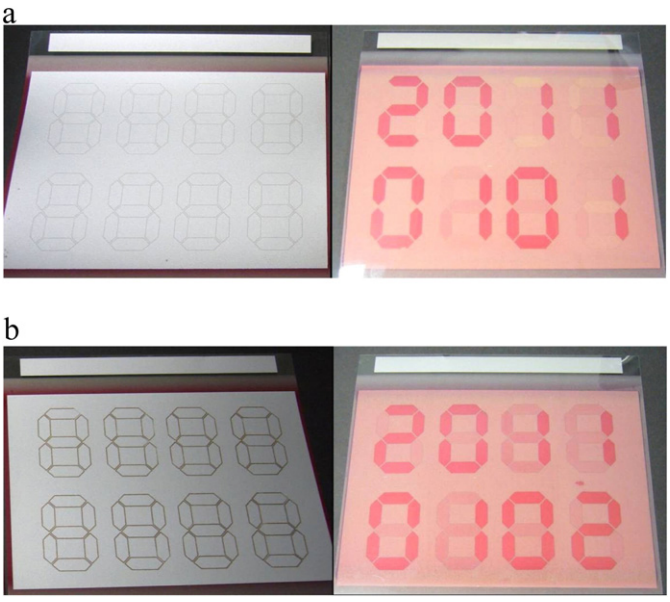

Fig. 6. Driving voltage results of Ch-LCD with silver electrode etched with (a) 1064 nm fiber laser and (b) 355 nm UV laser.

4. Conclusions

Both 1064 nm fiber laser and 355 nm solid-state laser can ablate the silver electrode layer of a Ch-LCD only and avoid injuring ITO electrode layer. Experiment results show that 1064 nm fiber laser processing reduces the damage to the liquid crystal layer and the underlying ITO layer, and decreases the heat-affected zone of the ablated electrode. For industrial application, the cost of a 1064 nm fiber laser is lower than that of a 355 nm solid-state laser. Using fiber laser processing to ablate the silver electrode improves throughput, lowers cost, and increases pattern quality.

Acknowledgement

The authors acknowledge the support from the Ministry of the Economic Affairs (MOEA), Taiwan, R.O.C.

References

[1] D.K. Yang, J. Disp. Technol. 2 (2006) 32.
[2] S.Y. Lu, L.C. Chien, Appl. Phys. Lett. 91 (2007) 131119.
[3] D.K. Yang, J.L. West, L.C. Chien, J.W. Doane, J. Appl. Phys. 76 (1994) 1331.
[4] X.J. Yu, H.S. Kwok, Appl. Phys. Lett. 85 (2004) 3711.
[5] A. Khan, T. Schneider, E. Montbach, D.J. Davis, N. Miller, D. Marhefka, T. Ernst, J.W. Doane, SID Int. Symp. Dig. Tech. Pap. 38 (2007) 54.
[6] T.J. White, R.L. Bricker, L.V. Natarajan, V.P. Tondiglia, C. Bailey, L. Green, Q. Li, T.J. Bunning, Opt. Commun. 283 (2010) 33434.
[7] M. Henry, P.M. Harrison, J. Wendland, SID Int. Symp. Dig. Tech. Pap. 38 (2007) 1209.
[8] G.T. McCollough, C.M. Rankin, M.L. Weiner, J. Soc. Inf. Display 14 (2006) 25.
[9] Y.H. Yoon, S.M. Yi, J.R. Yim, J.H. Lee, G. Rozgonyi, Y.C. Joo, Microelectron. Eng. 87 (2010) 2230.
[10] R. Lesyuk, W. Jillek, Y. Bobitski, B. Kotlyarchuk, Microelectron. Eng. 88 (2011) 318.
[11] M.F. Chen, Y.P. Chen, W.T. Hsiao, Z.P. Gu, Thin Solid Films 515 (2007) 8515.
[12] Z.H. Li, E.S. Cho, S.J. Kwon, Appl. Surf. Sci. 255 (2009) 9843.
[13] H. Lee, H. Shin, M. Lee, Opt. Lasers Eng. 48 (2010) 380.
[14] H.K. Lin, C.H. Li, S.H. Liu, Opt. Lasers Eng. 48 (2010) 1008.